Multi-tissue epigenetic analysis of the osteoarthritis susceptibility locus mapping to the plectin gene *PLEC*

A.K. Sorial[†*], I.M.J Hofer[†], M. Tselepi[†], K. Cheung[†], E. Parker[†], D.J. Deehan[‡], S.J. Rice[†], J. Loughlin[†*]

[†]Newcastle University, Biosciences Institute, Newcastle upon Tyne, UK

[‡]Freeman Hospital, Newcastle Upon Tyne, UK

Author email addresses:

Antony Sorial: tony.sorial@newcastle.ac.uk
Ines Hofer: ines.hofer@newcastle.ac.uk
Maria Tselepi: maria.tselepi@newcastle.ac.uk
Kathleen Cheung: kat.cheung@newcastle.ac.uk
Eleanor Parker: eleanor.parker@newcastle.ac.uk
David Deehan: david.deehan@newcastle.ac.uk
Sarah Rice: sarah.rice@newcastle.ac.uk
John Loughlin: john.loughlin@newcastle.ac.uk

[*]Address correspondence and reprint requests to:
Mr. Antony K. Sorial or Professor John Loughlin, Newcastle University, Biosciences Institute, International Centre for Life, Newcastle upon Tyne, NE1 3BZ, United Kingdom.
Tel: +44 (0)191 241 8988; Fax: +44 (0)191 241 8666. E-mail: tony.sorial@newcastle.ac.uk (A.K. Sorial), john.loughlin@newcastle.ac.uk (J. Loughlin)

Running headline: Epigenetic analysis of the *PLEC* OA risk locus

Objective

Osteoarthritis (OA) associated single nucleotide polymorphism (SNP) rs11780978 correlates with differential expression of *PLEC,* and methylation quantitative trait loci (mQTLs) at *PLEC* CpGs in cartilage. This implies that methylation links chondrocyte genotype and phenotype, thus driving the functional effect. *PLEC* encodes plectin, a cytoskeletal protein that enables tissues to respond to mechanical forces. We sought to assess whether *PLEC* functional effects were cartilage specific.

Method

Cartilage, fat pad, synovium and peripheral blood were collected from patients undergoing arthroplasty. *PLEC* CpGs were analysed for mQTLs and allelic expression imbalance (AEI) was performed. We focussed on previously reported mQTL clusters neighbouring cg19405177 and cg14598846. Plectin was knocked down in a mesenchymal stem cell (MSC) line using CRISPR/Cas9 and cells phenotyped by RNA-sequencing.

Results

Novel mQTLs were discovered in fat pad, synovium and peripheral blood at both clusters. The genotype-methylation effect of rs11780978 was stronger in cg14598846 than in cg19405177 and stronger in joint tissues than in peripheral blood. We observed AEI in synovium in the same direction as for cartilage. Knocking-down plectin impacted on pathways reported to have a role in OA, including Wnt signalling, glycosaminoglycan biosynthesis and immune regulation.

Conclusions

Synovium is also a target of the rs11780978 OA association functionally operating on *PLEC*. In fat pad, mQTLs were identified but these did not correlate with *PLEC* expression, suggesting the functional effect is not joint-wide. Our study highlights interplay between genetic risk, DNA methylation and gene expression in OA, and reveals clear differences between tissues from the same diseased joint.

Keywords: osteoarthritis, genetic risk, epigenetics, gene expression, *PLEC*, CRISPR/Cas9, cytoskeletal

Introduction

Osteoarthritis (OA) is an extremely common musculoskeletal disorder that is characterised by focal loss of articular cartilage leading to chronic pain, disability, co-morbidities including cardiovascular disease, and premature death[1-3]. OA is polygenic and in recent years over 90 genome-wide significant loci have been mapped in Europeans using high-density single nucleotide polymorphism (SNP) arrays[4-10]. An overwhelming majority of the associated polymorphisms reside in non-protein-coding regions of the genome and, as such, OA genetic susceptibility is presumed to act principally via changes to gene expression. The availability of excised tissue following arthroplasty of an OA joint offers the opportunity to experimentally test this in disease-relevant cells, including cartilage chondrocytes, the single cell type in this tissue[11]. As such, many OA risk alleles have been shown to correlate with alteration in the expression of nearby genes in chondrocytes[12]. These effects are known as expression quantitative trait loci (eQTLs). DNA methylation changes at CG dinucleotides (CpGs) also regulate gene expression and OA-associated SNPs have been shown to correlate with methylation levels in cartilage DNA in *cis*[13]. These effects are known as methylation QTLs (mQTLs). Furthermore, several OA risk loci correlate with both methylation and expression, with alteration of the former being shown experimentally to modulate the latter[14]. These effects are known as methylation and expression QTLs (meQTLs). Overall, these studies indicate that DNA methylation links chondrocyte genotype and phenotype, with this epigenetic mechanism underpinning and driving a large proportion of the functional impact of OA genetic risk. Furthermore, in most instances, OA mQTLs localize to predicted enhancers[13], placing OA in the "enhanceropathy" category of common diseases[15].

We previously reported that an OA association marked by SNP rs11780978 (G>A) correlated with methylation of nine CpGs measured using the Illumina Infinium HumanMethylation450 genome-wide CpG array[16]. The SNP and CpGs are all located within the *PLEC* gene on chromosome 8q24.3. We subsequently focused on two of the most significant CpGs from amongst the nine, cg19405177 and cg14598846, and by using pyrosequencing, we replicated the correlation between rs11780978 genotype and CpG methylation in an independent panel of DNAs. The two pyrosequencing assays used to replicate cg19405177 and cg14598846 captured an additional seven CpGs flanking cg19405177 and an additional three CpGs adjacent to cg14598846. The methylation of these additional CpGs also correlated with rs11780978 genotype. Furthermore, using allelic expression imbalance (AEI) analysis (a complementary approach to standard eQTL analysis[17])

we demonstrated that the OA risk-conferring A allele of rs11780978 correlated with reduced *PLEC* expression, and that expression of the gene also correlated with methylation at CpGs in the cg19405177 and cg14598846 clusters[16]. These mQTL, eQTL and meQTL studies were all performed on cartilage DNA and RNA, and highlighted *PLEC* as a target of the OA susceptibility mapping to chromosome 8q24.3.

PLEC encodes plectin, a large cytoskeletal protein that regulates signalling from the extracellular environment to the cell nucleus[18-19]. Plectin enables cells to respond to external mechanical stimuli and forces, such as those experienced by the chondrocyte during joint movement[20]. Although cartilage loss is central to the OA disease process, there are pathological changes to other tissues of the articulating joint that occur concurrent to and following the loss of cartilage[21]. *PLEC* is expressed widely and in this report, we set out to test whether the mQTL, eQTL and meQTL effects that we had discovered were cartilage specific or whether they were active in other joint or non-joint tissues. We also modelled the transcriptional effect that the OA risk-conferring allele of rs11780978 has on *PLEC* by knocking-down plectin in a mesenchymal stem cell line using CRISPR/Cas9 and assessing the impact on global gene expression.

Materials and Methods

OA Patients

Tissue samples were collected from patients undergoing knee or hip arthroplasty for primary OA at the Newcastle upon Tyne Foundation Trust hospitals. Ethical approval was granted by the Health Research Authority of the National Health Service (research ethics committee reference 14/NE/1212) and each donor provided verbal and written informed consent. We collected macroscopically normal cartilage (36 samples, distal from the lesion and avoiding areas of fibrillated tissue), infrapatellar fat pad (68 samples) and synovium (81 samples). For some patients, more than one joint tissue type was available for analysis. We also collected whole peripheral blood samples from 55 of the patients just prior to their surgery, using EDTA vacutainers for DNA extraction and Tempus™ tubes for RNA extraction (ThermoFisher Scientific). In total, we analysed tissue samples from 202 OA patients. Further patient details can be found in Supplementary Table 1.

100 **Nucleic acid extraction from tissue samples**

101 Joint tissue samples were stored frozen and ground to a powder using a mixermill (Retsch
102 Limited) under liquid nitrogen. For cartilage, RNA was extracted using TRIzol (Life
103 Technologies) and DNA was extracted using the E.Z.N.A. Tissue DNA isolation kit (Omega
104 Biotek, VWR). For fat pad and synovium, DNA and RNA were extracted using the E.Z.N.A.
105 DNA/RNA isolation kit (Omega Biotek, VWR). For blood, DNA was extracted using the
106 QIAamp DNA blood mini kit (Qiagen) and RNA was extracted using the Tempus^{TM} Spin RNA
107 isolation kit (ThermoFisher Scientific).

108

109 **Quantitative gene expression**

110 cDNA synthesis and quantitative PCR (qPCR) were performed as described previously[22].
111 Predesigned TaqMan assays (Integrated DNA Technologies) were used to quantify expression
112 of the housekeeping genes *HPRT1*, *18S* and *GAPDH*. For *PLEC,* expression primers were
113 designed using the Roche probe library system and are located in exons 19 and 20, which are
114 present in all isoforms of the gene (primers 5'-CTGCGTAGGAAATACAGTT-3' and 5'-
115 CAGCTGTTCCTTCTCGTCCT-3'). The relative expression of *PLEC* was calculated by the 2^{-}
116 $^{\Delta Ct}$ method, where ΔCt is the mean Ct value of the three housekeeping genes subtracted from
117 the Ct value of *PLEC*.

118

119 **mQTL and eQTL analysis**

120 Genotyping of association SNP rs11780978 and *PLEC* transcript SNP rs11783799 (A>G),
121 DNA methylation analysis at the cg19405177 and cg14598846 CpG clusters, and *PLEC* AEI
122 analysis using rs11783799 were all performed as described previously using the same protocols
123 and assays[16]. In the methylation analysis, PCRs were performed in duplicate on each sample
124 and the mean calculated, with samples being excluded from the analysis if the methylation
125 between the PCR replicates differed by >5%. In the AEI analysis, PCRs were performed in
126 triplicate on each tissue cDNA and DNA sample, with samples excluded from the analysis if
127 the values between the PCR replicates differed by >5%.

128

129 **Generation of a mesenchymal stem cell line constitutively expressing Cas9 (MSC-Cas9)**

130 We purchased the immortalised human mesenchymal stem cell (MSC) line SCRC-4000
131 (ATCC) and transduced it with the lentiCRISPR v2 plasmid 52961, which contains a Cas9
132 insert and confers puromycin resistance (Addgene). The cells were expanded in complete
133 growth medium consisting of serum free media (PCS-500-030, ATCC) supplemented with

134 Mesenchymal Stem Cell Growth Kit containing L-Alanyl-L-Glutamine (PCS-500-040,
135 ATCC), G418 disulphate salt solution (G8168, Sigma Aldrich) and penicillin-streptomycin
136 (30-2300, ATCC). Selection of Cas9 expressing cells was achieved by addition of 0.35ug/µl
137 of puromycin to the complete growth media. Constitutive expression of Cas9 was confirmed
138 by immunoblot with a Cas9 antibody (7A9-3A3, Cell Signalling Technology).
139
140 **CRISPR/Cas9**
141 CHOPCHOP (https://chopchop.cbu.uib.no/) was used to design guide RNA (gRNA) sequences
142 that would generate a 26bp frame-shift deletion of exon 3 of *PLEC* (primers 5'-
143 CTGTATGAAGACCTCCGCGA-3' and 5'-CCCCGAGAGGACCTCCAGCA-3'). This exon
144 is present in all isoforms of the gene. The gRNAs were then purchased as synthetic Alt-R®
145 CRISPR-Cas9 crRNAs alongside Alt-R® CRISPR-Cas9 tracrRNA (Integrated DNA
146 Technologies). MSC-Cas9 cells were plated at sub-confluence (45,000 cells/well) in 6-well
147 plates (VWR) and allowed to adhere for 24 hours. For deletions (4 replicates), paired crRNAs
148 were annealed to tracrRNA in a 1:1:2 ratio at 95ºC for 5 minutes, whilst for controls (4
149 replicates), tracrRNA alone was used. Deletion and control mixes were separately combined
150 with Dharmafect1 (Dharmacon) in serum free media (PCS-500-030, ATCC) to produce a
151 transfection mix. 200ul of media/well was aspirated and replaced with transfection mix for 24
152 hours, after which the media was changed to complete growth medium and the cells expanded
153 in T182.5 flasks (VWR) in monolayer and until confluent (between 10-14 days), with two
154 changes of media per week. Cells were detached by trypsinization, washed in phosphate-
155 buffered saline (PBS), spun and the cell pellets frozen. DNA, RNA and protein were
156 simultaneously extracted from pellets using the NucleoSpin TriPrep Kit (Macherey-Nagel,
157 supplied by ThermoFisher). Deletion of the target region was confirmed by end-point PCR of
158 DNA using primers flanking the guides (primers 5'-GAGGGGTTGAGCTGGATTCC-3' and
159 5'-CCAGCACCCACTCTGTAGAT-3') and by Sanger sequencing.
160
161 **Immunoblotting**
162 Up to 10µg of total protein was resolved on NuPAGE™ 3-8% Tris-Acetate Protein Gels
163 (Invitrogen) in 1x NuPAGE™ Tris-Acetate SDS Running Buffer (Invitrogen). Protein was
164 transferred through a semi-dry transfer at 200mA/gel for 3 hours. Blots were probed with anti-
165 plectin guinea pig polyclonal serum (GP21, Progen)/goat anti-guinea pig (AB6908, Abcam)

166 and anti-GAPDH (MAB374, Sigma Aldrich)/goat anti-mouse (P0447, Dako) as a loading
167 control.
168
169 **RNA-sequencing**
170 For each sample, the TruSeq Stranded mRNA library prep kit (Illumina) was used to prepare a
171 sequencing library from 1.5µg of total RNA. All samples were then sequenced to a depth of
172 ~52-71 million paired end reads on an Illumina NextSeq platform. Quality control of raw
173 sequencing reads was performed using FastQC (v0.11.7). All samples passed QC. Reads were
174 mapped to the hg38 (ENSEMBL version 91) reference genome using Salmon (v0.14.1) in
175 quasi-mapping mode on default settings[23]. All samples except one achieved alignment rates of
176 ~88%. Counts were summarised to gene level and imported into R using tximport[24]. Principle
177 component analysis (PCA) revealed the sample with the low alignment rate to be an outlier
178 and this was removed from further analysis, leaving four *PLEC* deletion and three controls.
179 Unwanted variation in the dataset was estimated using surrogate variable analysis (svaseq[25]).
180 The number of surrogate variables was estimated at two and these were included into the model
181 for differential expression analysis. Differential expression analysis between deletion and
182 control samples was performed using the Wald test implemented in DESeq2[26]. The false
183 discovery rate (FDR) was controlled using the Benjamini-Hochberg procedure. Genes with an
184 FDR $P<0.05$ were considered significant. Gene set enrichment analysis (GSEA[27]) was used to
185 discover overrepresented pathways in the set of up- and down-regulated genes. The full gene
186 list was ranked by signed log10(*P* value); positive sign if up-regulated and negative if down-
187 regulated. This pre-ranked list was used as input into the fgsea package in Bioconductor to
188 query enrichment of Reactome pathways[28]. Pathways with an FDR $P<0.25$ were considered
189 significant, as recommended by the developers of GSEA[27]. To visualise splice junctions, reads
190 were aligned to hg38 reference genome using STAR (v2.4.2a) short read aligner using default
191 settings[29] and viewed in Integrative Genomics Viewer (IGV[30]).
192
193 **Statistical analyses**
194 When correlating association between rs11780978 genotype and methylation of CpGs, *P*
195 values were calculated using the Kruskal-Wallis test. For comparison of global methylation
196 between tissues, Kruskal-Wallis with Dunn's multiple comparisons was used. For quantitative
197 *PLEC* expression analyses, *P* values were calculated using a Mann-Whitney 2-tailed exact test.
198 For *PLEC* AEI, *P* values were calculated using Wilcoxon's matched pairs signed rank test.

199 # Results

200 ***PLEC* cartilage mQTLs are present in other tissues**

201 We previously discovered *PLEC* mQTLs in cartilage DNA[16]. For cg19405177 and its seven
202 flanking CpGs (located in a 112bp interval), the OA risk-conferring A allele of rs11780978
203 correlated with increased methylation, whereas for cg14598846 and its three adjacent CpGs
204 (located in a 23bp interval), the A allele correlated with decreased methylation. In this report,
205 we first assessed if these mQTLs were also active in DNA from fat pad, synovium and blood.
206 We also included a new cohort of cartilage DNAs. Figure 1 provides the data for cg19405177
207 and cg14598846, whilst the data for all 12 CpGs across the four tissues can be found in
208 Supplementary Figures 1 (cartilage), 2 (fat pad), 3 (synovium) and 4 (blood). The mQTLs were
209 replicated in the new batch of cartilage DNAs and in the same directions as before. The mQTLs
210 were also present in the other tissues and also in the same direction.

211 When we plotted the methylation data by tissue type but independent of genotype, there
212 were significant differences in methylation levels (Supplementary Figure 5). For example,
213 cg19405177 demonstrated higher methylation values in fat pad and synovium compared to
214 cartilage and blood, whilst cg14598846 demonstrated higher methylation values in blood
215 compared to joint tissues. To emphasize this variability in CpG methylation in tissues from the
216 same patient, we plotted the cg19405177 and cg14598846 data for those patients in whom we
217 had studied two or more tissues. There were 18 such patients with data generated at
218 cg19405177 and 20 patients with data generated at cg14598846 (Figure 2). The variability in
219 methylation between the tissues of an individual is particularly clear for patient 6550 at
220 cg19405177, and patient 6599 at cg14598846, with a methylation range of >30% across the
221 four tissues tested for each CpG.

222 We next constructed heat maps of the percentage effect of rs11780978 genotype on
223 methylation at each CpG in each tissue. For cartilage, we included data from the replication
224 study of our previous report[16] to maximise power. For the cg19405177 CpGs, the average
225 genotypic effect for all eight CpGs combined was 31.3% in cartilage, 17.4% in fat pad, 21.2 %
226 in synovium and 9.3% in blood (Figure 3A). For the cg14598846 CpGs, the average genotypic
227 effect for all four CpGs combined were comparable across the joint tissues, with values of
228 85.0% in cartilage, 81.4% in fat pad and 87.5% in synovium (Figure 3B). Although the
229 genotypic effect in blood was lower, it was still high at 43.5%. At the individual CpG level,
230 there were some striking differences between tissues. For example, cg19405177 had a

231 genotypic effect of >30% in cartilage, synovium and blood but only 3.9% in fat pad. These
232 large differences imply intra-tissue differences in the nature of the mQTLs.
233 Overall, this analysis highlighted that the previously reported *PLEC* mQTLs are active
234 in non-cartilaginous tissues and that the effects are stronger in joint tissues than blood.
235 Although the genotypic effect of rs11780978 is greater in cartilage for the cg19405177 CpGs,
236 this is not the case for the cg14598846 CpGs.
237
238 **The *PLEC* rs11780978 eQTL is active in synovium**
239 Before testing for the *PLEC* rs11780978 eQTL by AEI analysis, we measured the relative
240 expression of the gene in fat pad, synovium and blood along with cartilage as a comparator
241 (Supplementary Figure 6). The qPCR data revealed that *PLEC* expression was equivalent
242 between cartilage and synovium, was higher in fat pad and lower in blood.
243 We performed AEI as described previously[16]. In summary, we identified rs11780978
244 heterozygotes who were also heterozygous for the *PLEC* transcript SNP rs11783799 (r^2=0.93;
245 the OA risk conferring A allele of rs11780978 correlates with the G allele of rs11783799). We
246 then used rs11783799 to quantify the relative allelic expression of *PLEC* in the compound
247 heterozygotes. The blood cDNA samples consistently failed quality control, with the PCR
248 replicates differing by >5% in all samples. This is likely a reflection of the lower expression of
249 *PLEC* in this tissue and we could not therefore generate blood AEI data. We were able to
250 generate AEI data for 19 fat pad and 20 synovium compound heterozygotes (Figure 4). AEI
251 was detectable in both tissues but only in synovium did the direction of AEI significantly
252 correlate with an allele of rs11783799, with reduced expression of *PLEC* correlating with the
253 G allele of the SNP in the combined analysis (P=0.0054; Figure 4B). In fat pad, AEI was
254 observed in a majority of the patients, but this did not correlate with a particular allele (P=0.31;
255 Figure 4A).
256 To emphasize the variability of AEI in tissues from the same patient, we next plotted
257 the data for those patients in whom we had studied fat pad and synovium (Supplementary
258 Figure 7). There were six such patients with clear variability in the G/A ratio between the two
259 tissues tested for most of these, with patients 5680 and 5725 demonstrating particularly clear
260 inter-tissue variability in the ratio; in both, the G allele is more highly expressed in fat pad but
261 more lowly expressed in synovium relative to the A allele.
262 The significant AEI in synovium was in the same direction that we had observed in
263 cartilage[16], with the G allele of rs11783799, which marks the OA risk conferring A allele of
264 rs11780978, demonstrating reduced *PLEC* expression. In that previous report, we had studied

265 19 cartilage compound heterozygotes and the mean G/A ratio was 0.89. The mean synovium
266 G/A ratio we detected here was 0.92.
267 We next plotted the *PLEC* AEI data for the fat pad and synovium compound
268 heterozygotes against their individual methylation data. In fat pad, there was no evidence of a
269 significant correlation between methylation and AEI at cg19405177, cg14598846 or the
270 additional 10 CpGs measured (all *P* values >0.05; Supplementary Figure 8). However, in
271 synovium, three of the CpGs correlated with AEI; CpG3 from the cg19405177 cluster
272 (*P*=0.049), and cg14598846 (*P*=0.039) and CpG2 (*P*=0.047) from the cg14598846 cluster
273 (Supplementary Figure 9). These three CpGs had also shown meQTL activity in our previous
274 cartilage study[16]. For CpG3 from the cg19405177 cluster, the same direction of effect is seen
275 in cartilage and synovium, with increased methylation correlating with decreased AEI (the $\log_2$
276 AEI ratio moves towards zero with increasing methylation). However, for cg14598846 and
277 CpG2 from the cg14598846 cluster, the effects are in opposite directions between cartilage and
278 synovium; in cartilage, increased methylation correlated with decreased AEI whereas in
279 synovium, increased methylation correlated with increased AEI (the $\log_2$ AEI ratio moves
280 away from zero with increasing methylation).
281 In summary, the *PLEC* rs11780978 eQTL previously observed in cartilage also
282 operates in synovium. Furthermore, we observed correlations between *PLEC* expression and
283 CpG methylation in synovium. These meQTLs are shared with cartilage but are not necessarily
284 operating in the same manner.
285
286 **Knock-down of *PLEC* and plectin elicits a response**
287 Our previous data and the results generated here highlight that the OA risk conferring A allele
288 of rs11780978 correlates with decreased expression of *PLEC* in cartilage and synovium. We
289 modelled this effect by knocking-down plectin. We used an immortalised human MSC cell line
290 that is amenable to CRISPR-based editing[31] and transduced it to constitutively express Cas9.
291 We then generated a 26bp frame-shift deletion of *PLEC* exon 3, with four replicates for deletion
292 and four control replicates. The cells were cultured in monolayer for up to 14 days and the
293 deletion was confirmed by PCR and Sanger sequencing, whilst a near-total plectin knock-out
294 was observed by immunoblotting using an antibody that binds to the C-terminus of the protein
295 (Figure 5A-C). The isolated RNA was then subjected to next-generation mRNA sequencing.
296 This revealed alternate splicing occurring in *PLEC* in the deletion samples, with exon 3 being
297 completely skipped in a subset of transcripts (Figure 5D). No exon skipping was seen in the
298 control samples. The level of *PLEC* mRNA was 26% lower in the deletion samples compared

299 to the controls (log_2 fold change of -0.44; FDR P=0.001; Supplementary Table 2). In summary,
300 this data implies that the Cas9-mediated deletion impacted on the transcription of *PLEC* and
301 on the translation of *PLEC* mRNA into plectin.

302 We next assessed the effect of this plectin knock-down on the transcriptome. In addition
303 to *PLEC*, the deletion had a significant effect (FDR P<0.05) on the expression of 269 genes
304 (Figure 6A and B, Supplementary Table 2). Pathway analysis revealed upregulation of
305 processes involving immune regulation and protein post-translation modification (Figure 6C),
306 and downregulation of Wnt signalling, metabolic pathways and glycosaminoglycan
307 biosynthesis, amongst others (Figure 6D). In conclusion, this model system highlighted that
308 depletion of *PLEC* and plectin impacted upon a range of pathways reported to play a critical
309 role in cartilage biology and OA.

310

311 **Discussion**

312 The mapping of risk loci for polygenic traits is now a relatively straightforward procedure,
313 with the next major step in complex trait analysis being the transition from association signal
314 to functional characterization[32]. For OA, considerable strides have been made in this regard in
315 recent years[33-35]. Our interest is in the epigenetic dimension of OA genetic risk and especially
316 the role of DNA methylation. This is the best characterized and most stable epigenetic
317 modification and modulates gene expression by disrupting the binding of transcription factors
318 and by facilitating the binding of methyl-binding proteins, which initiate compaction of
319 chromatin and gene silencing[36]. Last year, we demonstrated that the OA association signal
320 marked by SNP rs11780978 correlated with methylation of CpGs within *PLEC* and with
321 variable expression of the gene[16]. These analyses were chondro-centric and here, we set out to
322 determine whether these functional effects were more widespread. If so, an exclusive focus on
323 cartilage as a target tissue of the rs11780978 association signal would not be merited.

324 We discovered that the rs11780978-*PLEC* eQTLs, mQTLs and meQTLs that are active
325 in cartilage are also active in synovium, but with some differences; the genotypic effect is
326 substantially greater in cartilage for the cg19405177 cluster of CpGs, whilst the cg14598846
327 meQTLs act in opposite directions between the two tissues. In fat pad, we observed the mQTLs
328 but *PLEC* AEI did not correlate with rs11780978 genotype. Instead, the OA risk-conferring A
329 allele of rs11780978 demonstrated increased and decreased expression relative to the non-risk
330 allele across the 19 fat pad samples studied, with no overall significant difference when the
331 data was combined. There are therefore eQTLs operating on *PLEC* in fat pad, but these are
332 unrelated to rs11780978. These distinctions point toward regulatory variability in gene

333 expression mediated by the same association between joint tissues. In blood, the mQTLs were
334 detectable but their genotypic effect was much weaker in comparison to the three joint tissues.
335 Such variable strengths of mQTLs effects between cells from different lineages are expected[37].
336 We were unable to test blood for *PLEC* eQTLs due to the low expression level of the gene. In
337 summary, we observed the *PLEC* mQTLs across all four tissues tested with the joint tissues
338 more similar to each other than to blood. This was exemplified by the mQTL genotypic effects
339 being much stronger in joint tissues. Since synovium was subject to eQTLs and meQTLs, it
340 too should be investigated as a target of the rs11780978 association signal.

341 Finally, we modelled the effect of the rs11780978 risk-conferring allele by knocking
342 down plectin in a cell line. *PLEC* mRNA was detectable in the RNA-sequencing data but at a
343 significantly lower level compared to control. The knock-down was very efficient at the protein
344 level, with a near total absence of plectin observed. The knock-down impacted on a range of
345 cellular pathways. Of particular note, both the innate and the acquired immune response
346 showed an upregulation, an effect that has been reported on previously in OA for both cartilage
347 and synovium[38-39]. Downregulation of Wnt signalling was also of interest, as this pathway is
348 critical to cartilage homeostasis[33,40]. Furthermore, there is growing evidence of an interplay
349 between Wnt signalling and inflammation in joint tissues[41]. Our model system did not include
350 mechanical load, a force which plectin allows cells to respond to[18-20]. Aberrant mechanical
351 load, including only moderate change, can elicit an inflammatory response that has been termed
352 "mechanoflammation"[42]. Our data suggests that even in the absence of load, the loss of plectin
353 is eliciting this response. A future model incorporating load may therefore reveal yet more
354 insight into a potential key role of plectin as a regulator of inflammation in response to
355 mechanical load and joint tissue injury in OA.

356 In conclusion, our investigations have highlighted the interplay between OA genetic
357 risk, DNA methylation and gene expression, and reveal clear differences in these effects for
358 tissues from the same diseased joint. Furthermore, by recapitulating the effect of the risk locus
359 at *PLEC*, we have linked OA genetic susceptibility with a number of cellular pathways, thus
360 providing mechanistic insight into OA aetiology.
361
362
363
364
365

366 **References**

367 1. Glyn-Jones S, Palmer AJ, Agricola R, Price AJ, Vincent TL, Weinans H, et al.
368 Osteoarthritis. Lancet 2015; 386: 376-387.
369 2. Kendzerska T, Juni P, King LK, Croxford R, Stanaitis I, Hawker GA. The longitudinal
370 relationship between hand, hip and knee osteoarthritis and cardiovascular events: a
371 population-based cohort study. Osteoarthritis Cartilage 2017; 25: 1771-1780.
372 3. Hawker GA, Croxford R, Bierman AS, Harvey PJ, Ravi B, Stanaitis I, et al. All-cause
373 mortality and serious cardiovascular events in people with hip and knee osteoarthritis: a
374 population based cohort study. PLoS One 2014; 9: e91286.
375 4. arcOGEN Consortium, arcOGEN Collaborators, Zeggini E, Panoutsopoulou K, Southam
376 L, Rayner NW, et al. Identification of new susceptibility loci for osteoarthritis (arcOGEN):
377 a genome-wide association study. Lancet 2012; 380: 815-823.
378 5. Reynard LN. Analysis of genetics and DNA methylation in osteoarthritis: What have we
379 learnt about the disease? Semin Cell Dev Biol 2017; 62: 57-66.
380 6. Styrkarsdottir U, Helgason H, Sigurdsson A, Norddahl GL, Agustsdottir AB, Reynard LN,
381 et al. Whole-genome sequencing identifies rare genotypes in COMP and CHADL
382 associated with high risk of hip osteoarthritis. Nat Genet 2017; 49: 801-805.
383 7. Zengini E, Hatzikotoulas K, Tachmazidou I, Steinberg J, Hartwig FP, Southam L, et al.
384 Genome-wide analyses using UK Biobank data provide insights into the genetic
385 architecture of osteoarthritis. Nat Genet 2018; 50: 549-558.
386 8. Styrkarsdottir U, Lund SH, Thorleifsson G, Zink F, Stefansson OA, Sigurdsson JK, et al.
387 Meta-analysis of Icelandic and UK data sets identifies missense variants in SMO, IL11,
388 COL11A1 and 13 more new loci associated with osteoarthritis. Nat Genet 2018; 50: 1681-
389 1687.

390 9. Tachmazidou I, Hatzikotoulas K, Southam L, Esparza-Gordillo J, Haberland V, Zheng J,
391 et al. Identification of new therapeutic targets for osteoarthritis through genome-wide
392 analyses of UK Biobank data. Nat Genet 2019; 51: 230-236.
393 10. Styrkarsdottir U, Stefansson OA, Gunnarsdottir K, Thorleifsson G, Lund SH, Stefansdottir
394 L, et al. GWAS of bone size yields twelve loci that also affect height, BMD, osteoarthritis
395 or fractures. Nat Commun 2019; 10: 2054.
396 11. den Hollander W, Pulyakhina I, Boer C, Bomer N, van der Breggen R, Arindrarto W, et al.
397 Annotating Transcriptional Effects of Genetic Variants in Disease-Relevant Tissue:
398 Transcriptome-Wide Allelic Imbalance in Osteoarthritic Cartilage. Arthritis Rheumatol
399 2019; 71: 561-570.
400 12. Shepherd C, Reese AE, Reynard LN, Loughlin J. Expression analysis of the osteoarthritis
401 genetic susceptibility mapping to the matrix Gla protein gene MGP. Arthritis Res Ther
402 2019; 21: 149.
403 13. Rice SJ, Cheung K, Reynard LN, Loughlin J. Discovery and analysis of methylation
404 quantitative trait loci (mQTLs) mapping to novel osteoarthritis genetic risk signals.
405 Osteoarthritis Cartilage 2019; 27: 1545-1556.
406 14. Reynard LN, Bui C, Syddall CM, Loughlin J. CpG methylation regulates allelic expression
407 of GDF5 by modulating binding of SP1 and SP3 repressor proteins to the osteoarthritis
408 susceptibility SNP rs143383. Hum Genet 2014; 133: 1059-1073.
409 15. Smith E, Shilatifard A. Enhancer biology and enhanceropathies. Nat Struct Mol Biol 2014;
410 21: 210-219.
411 16. Rice SJ, Tselepi M, Sorial AK, Aubourg G, Shepherd C, Almarza D, et al. Prioritization of
412 PLEC and GRINA as Osteoarthritis Risk Genes Through the Identification and
413 Characterization of Novel Methylation Quantitative Trait Loci. Arthritis Rheumatol 2019;
414 71: 1285-1296.

415 17. Pastinen T. Genome-wide allele-specific analysis: insights into regulatory variation. Nat
416 Rev Genet 2010; 11: 533-538.
417 18. Castanon MJ, Walko G, Winter L, Wiche G. Plectin-intermediate filament partnership in
418 skin, skeletal muscle, and peripheral nerve. Histochem Cell Biol 2013; 140: 33-53.
419 19. Rezniczek GA, Winter L, Walko G, Wiche G. Functional and Genetic Analysis of Plectin
420 in Skin and Muscle. Methods Enzymol 2016; 569: 235-259.
421 20. Goldmann WH. Intermediate filaments and cellular mechanics. Cell Biol Int 2018; 42: 132-
422 138.
423 21. Loeser RF, Goldring SR, Scanzello CR, Goldring MB. Osteoarthritis: a disease of the joint
424 as an organ. Arthritis Rheum 2012; 64: 1697-1707.
425 22. Gee F, Rushton MD, Loughlin J, Reynard LN. Correlation of the osteoarthritis
426 susceptibility variants that map to chromosome 20q13 with an expression quantitative trait
427 locus operating on NCOA3 and with functional variation at the polymorphism
428 rs116855380. Arthritis Rheumatol 2015; 67: 2923-2932.
429 23. Patro R, Duggal G, Love MI, Irizarry RA, Kingsford C. Salmon provides fast and bias-
430 aware quantification of transcript expression. Nat Methods 2017; 14: 417-419.
431 24. Soneson C, Love MI, Robinson MD. Differential analyses for RNA-seq: transcript-level
432 estimates improve gene-level inferences. F1000Res 2015; 4: 1521.
433 25. Leek JT. svaseq: removing batch effects and other unwanted noise from sequencing data.
434 Nucleic Acids Res 2014; 42.
435 26. Love MI, Huber W, Anders S. Moderated estimation of fold change and dispersion for
436 RNA-seq data with DESeq2. Genome Biol 2014; 15: 550.
437 27. Subramanian A, Tamayo P, Mootha VK, Mukherjee S, Ebert BL, Gillette MA, et al. Gene
438 set enrichment analysis: a knowledge-based approach for interpreting genome-wide
439 expression profiles. Proc Natl Acad Sci U S A 2005; 102: 15545-15550.

440 28. Croft D, O'Kelly G, Wu G, Haw R, Gillespie M, Matthews L, et al. Reactome: a database
441 of reactions, pathways and biological processes. Nucleic Acids Res 2011; 39: D691-697.
442 29. Dobin A, Davis CA, Schlesinger F, Drenkow J, Zaleski C, Jha S, et al. STAR: ultrafast
443 universal RNA-seq aligner. Bioinformatics 2013; 29: 15-21.
444 30. Thorvaldsdottir H, Robinson JT, Mesirov JP. Integrative Genomics Viewer (IGV): high-
445 performance genomics data visualization and exploration. Brief Bioinform 2013; 14: 178-
446 192.
447 31. Farhang N, Brunger JM, Stover JD, Thakore PI, Lawrence B, Guilak F, et al. (*) CRISPR-
448 Based Epigenome Editing of Cytokine Receptors for the Promotion of Cell Survival and
449 Tissue Deposition in Inflammatory Environments. Tissue Eng Part A 2017; 23: 738-749.
450 32. Gallagher MD, Chen-Plotkin AS. The Post-GWAS Era: From Association to Function. Am
451 J Hum Genet 2018; 102: 717-730.
452 33. Monteagudo S, Cornelis FMF, Aznar-Lopez C, Yibmantasiri P, Guns LA, Carmeliet P, et
453 al. DOT1L safeguards cartilage homeostasis and protects against osteoarthritis. Nat
454 Commun 2017; 8: 15889.
455 34. Shepherd C, Zhu D, Skelton AJ, Combe J, Threadgold H, Zhu L, et al. Functional
456 Characterization of the Osteoarthritis Genetic Risk Residing at ALDH1A2 Identifies
457 rs12915901 as a Key Target Variant. Arthritis Rheumatol 2018; 70: 1577-1587.
458 35. Klein JC, Keith A, Rice SJ, Shepherd C, Agarwal V, Loughlin J, et al. Functional testing
459 of thousands of osteoarthritis-associated variants for regulatory activity. Nat Commun
460 2019; 10: 2434.
461 36. Zhu H, Wang G, Qian J. Transcription factors as readers and effectors of DNA methylation.
462 Nat Rev Genet 2016; 17: 551-565.

463 37. Smith AK, Kilaru V, Kocak M, Almli LM, Mercer KB, Ressler KJ, et al. Methylation
464 quantitative trait loci (meQTLs) are consistently detected across ancestry, developmental
465 stage, and tissue type. BMC Genomics 2014; 15: 145.
466 38. Berenbaum F, van den Berg WB. Inflammation in osteoarthritis: changing views.
467 Osteoarthritis Cartilage 2015; 23: 1823-1824.
468 39. Miller RJ, Malfait AM, Miller RE. The innate immune response as a mediator of
469 osteoarthritis pain. Osteoarthritis Cartilage 2019.
470 40. Monteagudo S, Lories RJ. Cushioning the cartilage: a canonical Wnt restricting matter. Nat
471 Rev Rheumatol 2017; 13: 670-681.
472 41. Claudel M, Jouzeau JY, Cailotto F. Secreted Frizzled-related proteins (sFRPs) in osteo-
473 articular diseases: much more than simple antagonists of Wnt signaling? FEBS J 2019;
474 286: 4832-4851.
475 42. Vincent TL. Mechanoflammation in osteoarthritis pathogenesis. Semin Arthritis Rheum
476 2019; 49: S36-S38.
477

478 **Author Contributions**

479 AKS and JL designed the study. AKS, IMJH, MT and SJR generated the experimental data.
480 AKS, IMJH, KC and EP analysed the data and prepared the manuscript figures. AKS, IMH,
481 and JL prepared the main manuscript text. DJD provided patient samples for analyses. All
482 authors were involved in drafting the article or revising it critically for intellectual content, and
483 all authors approved the final version to be published.
484

485 **Acknowledgements**

486 Dr Colin Shepherd provided input into data interpretation and reviewed the manuscript.
487

488 **Funding**

489 This work was supported by Versus Arthritis (grant 20771) and by the Medical Research
490 Council and Versus Arthritis as part of the Centre for Integrated Research into Musculoskeletal
491 Ageing (CIMA, grant references JXR 10641, MR/P020941/1 and MR/R502182/1). Funds to

purchase the pyrosequencer were provided by The Ruth and Lionel Jacobson Charitable Trust, which also supported EP. AKS was funded by the Royal College of Surgeons of Edinburgh Cutner Fellowship and The John George William Patterson (JGWP) Foundation, IMJH was funded by JGWP.

Competing interest

The authors declare that they have no competing interests.

Data Availability

All data are available from the corresponding authors upon request. Raw RNA-seq data has been deposited into the NCBI GEO datasets repository with accession number GSE143725.

Legends to figures

Figure 1. Association between rs11780978 genotype and methylation at CpGs cg19405177 and cg14598846 in cartilage, fat pad, synovium and blood DNA. *P* values were calculated using the Kruskal-Wallis test. Horizontal lines and error bars show the mean ± SEM.
n = the number of patients providing data per CpG site for each tissue.

Figure 2. Differences in methylation within tissues of the same patient. Methylation at CpGs cg19405177 (**A**) and cg14598846 (**B**) were plotted for those individuals in whom methylation data was generated for two or more tissues. Numbers on the x-axis refer to the anonymised identification number assigned to patients at recruitment. Data is grouped by genotype at rs11780978.

Figure 3. Heat maps displaying the percentage effect of genotype at rs11780978 upon methylation at CpG clusters cg19405177 (**A**) and cg14598846 (**B**) for the four patient tissues. The correlation between genotype and methylation was determined using adjusted r^2 values calculated using a standard least squares linear regression model and expressed as a percentage. Data analysis was performed using SAS JMP Statistical Data Visualization Software and heat maps produced in PRISM. Patients contributing data to the cg19405177 cluster 1: cartilage, n=81; fat pad, n=39; synovium, n=64; blood, n=43. Patients contributing data to the cg14598846 cluster: cartilage, n=103; fat pad, n=68; synovium, n=79; blood, n=54.

525 **Figure 4.** *PLEC* allelic expression imbalance (AEI) in fat-pad (**A**) and synovium (**B**). AEI
526 analysis was conducted using transcript SNP rs11783799. The risk/non-risk allelic ratio is
527 plotted, with a ratio <1 indicating decreased *PLEC* expression from the risk allele. For each
528 patient, the mean of the DNA ratio (black, n=3 technical repeats) and the mean of the cDNA
529 ratio (grey, n=3 technical repeats) is plotted. Numbers on the x-axis refer to the anonymised
530 identification number assigned to patients at recruitment. The values for DNA and cDNA for
531 all patients combined are represented as box plots to the right, in which the lines within the box
532 represent the median, the box represents the 25th to 75th percentile, and the whiskers represent
533 the maximum and minimum values. *P* values were calculated using Wilcoxon's matched pairs
534 signed rank test.
535
536 **Figure 5.** Knock-down of plectin using CRISPR/Cas9. (**A**) The 26bp sequence of *PLEC* exon
537 3 deleted. (**B**) Representative agarose gel image showing the PCR product for control (non-
538 deleted) and deletion. (**C**) Representative immunoblot comparing plectin levels in control
539 versus deletion, with GAPDH as a loading control. (**D**) Sashimi plot showing splicing of
540 merged *PLEC* deletion (red) and control (blue) samples. Data were viewed on IGV genome
541 browser. The multiple isoforms of *PLEC* are shown on the bottom of the panel. Read coverages
542 show the presence of reads within exons. The lines illustrate the splicing between exons. The
543 values on the lines show the number of junction spanning reads. The merged deletion track
544 shows the absence of the 26bp region deleted within *PLEC* exon 3 (indicated by the box).
545
546 **Figure 6.** Differentially expressed genes and pathways. (**A**) Volcano plot illustrating
547 significantly differentially expressed genes between *PLEC* deletion and control samples. The
548 x-axis shows the $\log_2$ fold change between condition and the y-axis shows the $-\log_{10}$(FDR).
549 Genes with an FDR $P<0.05$ are shown in red. (**B**) Heatmap of significantly differentially
550 expressed genes between *PLEC* deletion and control. Normalised counts were used for plotting.
551 Hierarchical clustering was used to cluster samples and genes. The heatmap shows that samples
552 cluster by condition (D0-Del, deletions; D0-Neg, controls). (**C**) Top 25 significantly
553 upregulated Reactome pathways found using GSEA. (**D**) Top 25 significantly downregulated
554 Reactome pathways found using GSEA. All genes were ranked using signed $\log_{10}$(*P*-value)
555 and this pre-ranked list used as input into GSEA to query enrichment of Reactome pathways.
556
557 **Supplementary Figure 1.** Association between rs11780978 genotype and methylation at CpG
558 clusters cg19405177 (**A**) and cg14598846 (**B**) in cartilage DNA. *P* values were calculated using

559 the Kruskal-Wallis test. Horizontal lines and error bars show the mean ± SEM. n = the number
560 of patients providing data per CpG site.
561
562 **Supplementary Figure 2.** Association between rs11780978 genotype and methylation at CpG
563 clusters cg19405177 (**A**) and cg14598846 (**B**) in fat pad DNA. *P* values were calculated using
564 the Kruskal-Wallis test. Horizontal lines and error bars show the mean ± SEM. n = the number
565 of patients providing data per CpG site.
566
567 **Supplementary Figure 3.** Association between rs11780978 genotype and methylation at CpG
568 clusters cg19405177 (**A**) and cg14598846 (**B**) in synovium DNA. *P* values were calculated
569 using the Kruskal-Wallis test. Horizontal lines and error bars show the mean ± SEM. n = the
570 number of patients providing data per CpG site.
571
572 **Supplementary Figure 4.** Association between rs11780978 genotype and methylation at CpG
573 clusters cg19405177 (**A**) and cg14598846 (**B**) in blood DNA. *P* values were calculated using
574 the Kruskal-Wallis test. Horizontal lines and error bars show the mean ± SEM. n = the number
575 of patients providing data per CpG site.
576
577 **Supplementary Figure 5.** Methylation at CpG clusters cg19405177 (**A**) and cg14598846 (**B**)
578 for the four patient tissues without stratification by rs11780978 genotype. *P* values were
579 calculated using Kruskal-Wallis with Dunn's multiple comparisons. Horizontal lines and error
580 bars show the mean ± SEM. n = the number of patients providing data per tissue and at each
581 CpG site. *$P \leq 0.05$; **$P \leq 0.01$; ***$P \leq 0.001$ ****$P \leq 0.0001$.
582
583 **Supplementary Figure 6.** Expression of *PLEC* in tissue samples from OA patients. *PLEC*
584 mRNA levels were measured by qPCR in cartilage (n=10), fat pad (n=9), synovium (n=10)
585 and blood (n=10). Horizontal lines and error bars show the mean ± SEM. *P* values were
586 calculated using a Mann-Whitney 2-tailed exact test. **$P \leq 0.01$; ***$P \leq 0.001$
587
588 **Supplementary Figure 7.** The six patients with AEI data for fat pad (FP) and synovium
589 (SYN). The risk/non-risk allelic ratio is plotted, with a ratio <1 indicating decreased *PLEC*
590 expression from the risk allele. For each patient, the mean of the DNA ratio (black, n=3
591 technical repeats) and the mean of the cDNA ratio (grey, n=3 technical repeats) is plotted.

592 Numbers on the x-axis refer to the anonymised identification number assigned to patients at
593 recruitment.
594
595 **Supplementary Figure 8.** Methylation expression quantitative trait locus analyses in fat pad.
596 *PLEC* $\log_2$ allelic expression imbalance (AEI) ratios were plotted against methylation at all
597 CpGs in the cg19405177 (**A**) and cg14598846 (**B**) clusters. The square of the correlation
598 coefficient (r^2) and *P* values were calculated by linear regression analysis using a standard least
599 squares model.
600
601 **Supplementary Figure 9.** Methylation expression quantitative trait locus analyses in
602 synovium. *PLEC* $\log_2$ allelic expression imbalance (AEI) ratios were plotted against
603 methylation at all CpGs in the cg19405177 (**A**) and cg14598846 (**B**) clusters. The square of
604 the correlation coefficient (r^2) and *P* values were calculated by linear regression analysis using
605 a standard least squares model.

Figure 1

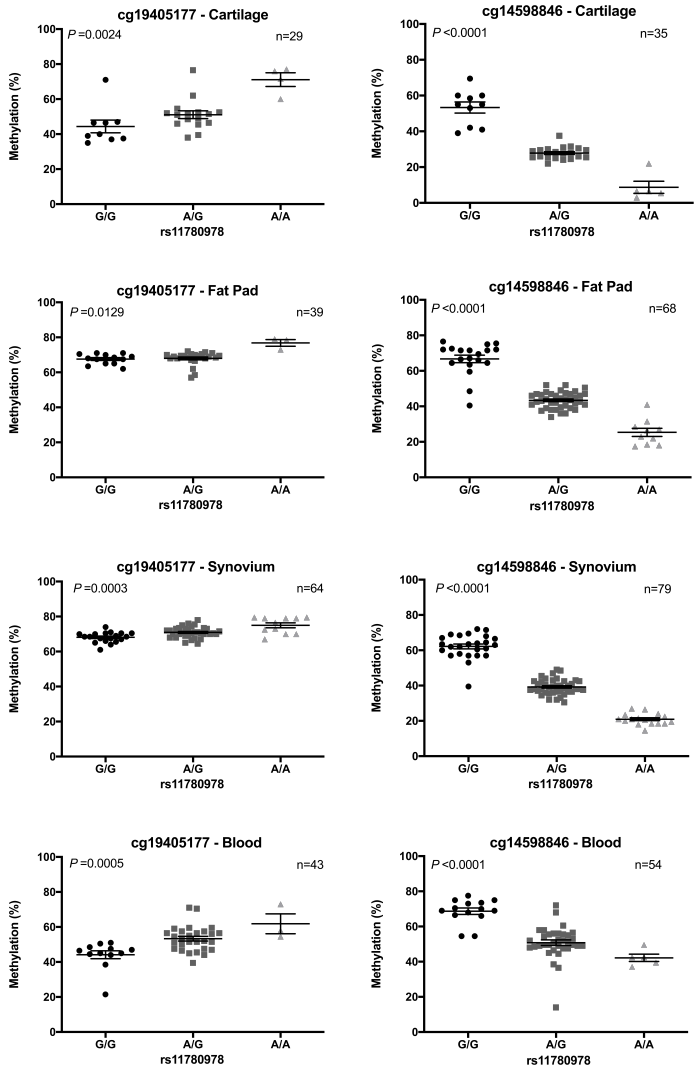
cg19405177 - Cartilage
P =0.0024
n=29
cg14598846 - Cartilage
P <0.0001
n=35
cg19405177 - Fat Pad
P =0.0129
n=39
cg14598846 - Fat Pad
P <0.0001
n=68
cg19405177 - Synovium
P =0.0003
n=64
cg14598846 - Synovium
P <0.0001
n=79
cg19405177 - Blood
P =0.0005
n=43
cg14598846 - Blood
P <0.0001
n=54
Methylation (%)
0
20
40
60
80
100
G/G
A/G
A/A
rs11780978

Figure 2

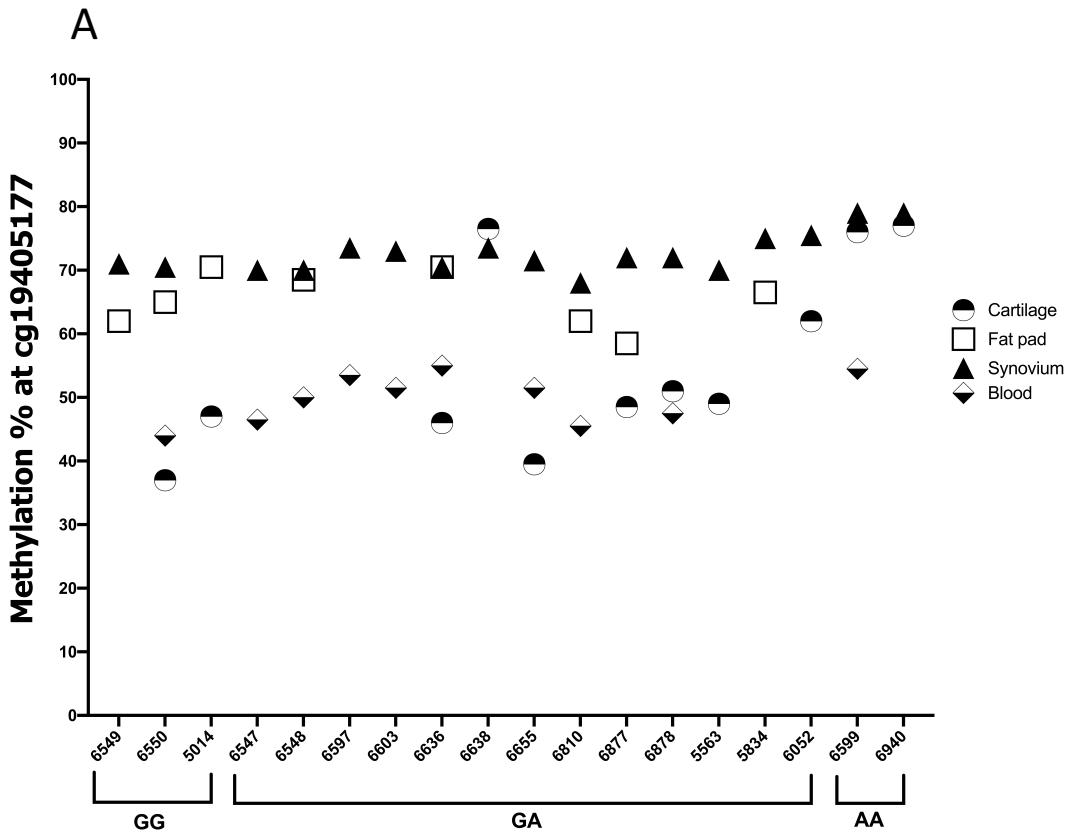
A
Methylation % at cg19405177
100
90
80
70
60
50
40
30
20
10
0
6549
6550
5014
6547
6548
6597
6603
6636
6638
6655
6810
6877
6878
5563
5834
6052
6599
6940
GG
GA
AA
Cartilage
Fat pad
Synovium
Blood

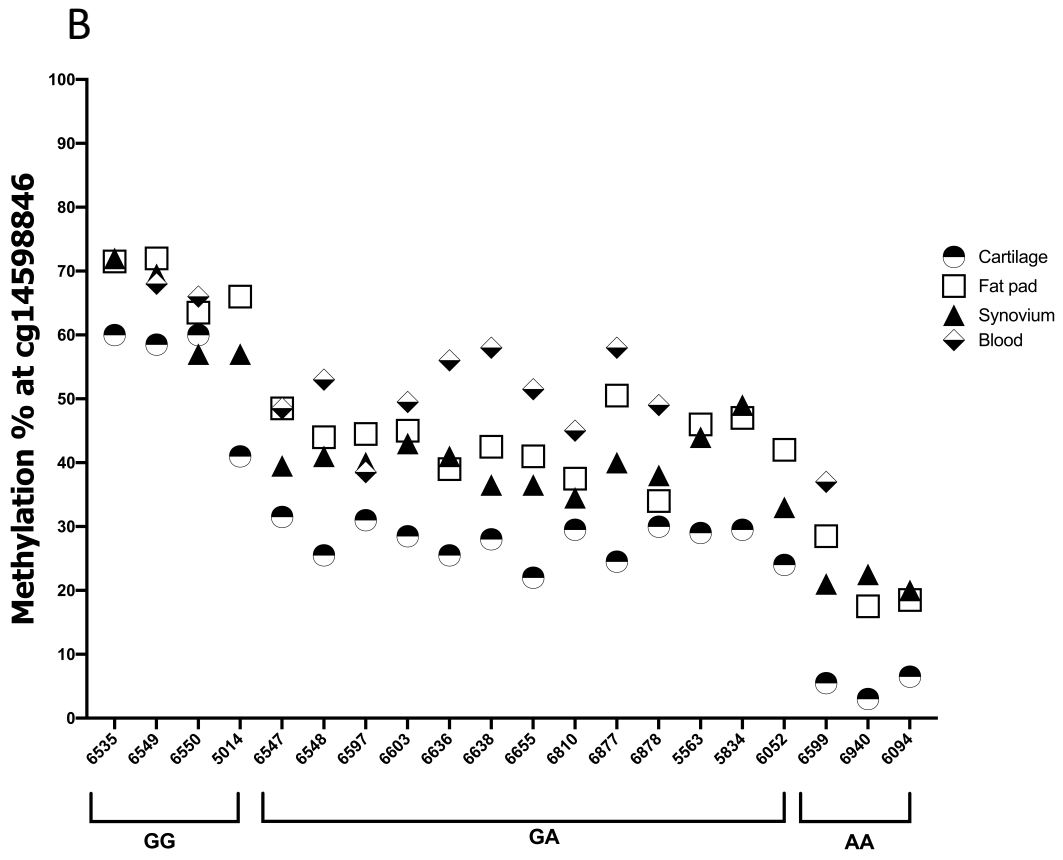
B
Methylation % at cg14598846
100
90
80
70
60
50
40
30
20
10
0
6535
6549
6550
5014
6547
6548
6597
6603
6636
6638
6655
6810
6877
6878
5563
5834
6052
6599
6940
6094
GG
GA
AA
Cartilage
Fat pad
Synovium
Blood

Figure 3

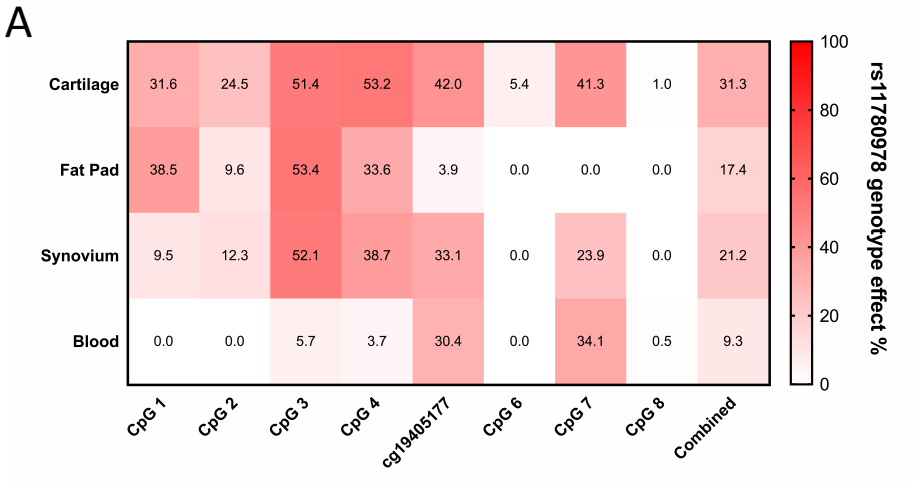
A
Cartilage
Fat Pad
Synovium
Blood
31.6 24.5 51.4 53.2 42.0 5.4 41.3 1.0 31.3
38.5 9.6 53.4 33.6 3.9 0.0 0.0 0.0 17.4
9.5 12.3 52.1 38.7 33.1 0.0 23.9 0.0 21.2
0.0 0.0 5.7 3.7 30.4 0.0 34.1 0.5 9.3
CpG 1
CpG 2
CpG 3
CpG 4
cg19405177
CpG 6
CpG 7
CpG 8
Combined
100
80
60
40
20
0
rs11780978 genotype effect %

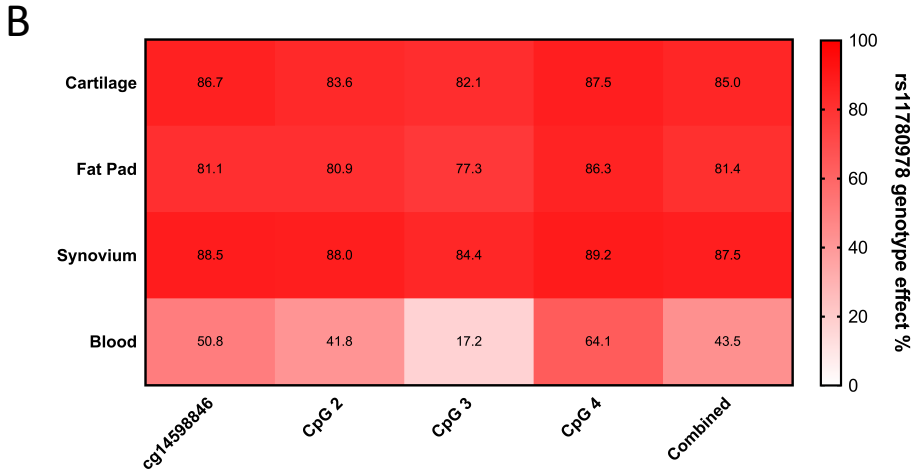
B
Cartilage
Fat Pad
Synovium
Blood
86.7 83.6 82.1 87.5 85.0
81.1 80.9 77.3 86.3 81.4
88.5 88.0 84.4 89.2 87.5
50.8 41.8 17.2 64.1 43.5
cg14598846
CpG 2
CpG 3
CpG 4
Combined
100
80
60
40
20
0
rs11780978 genotype effect %

Figure 4

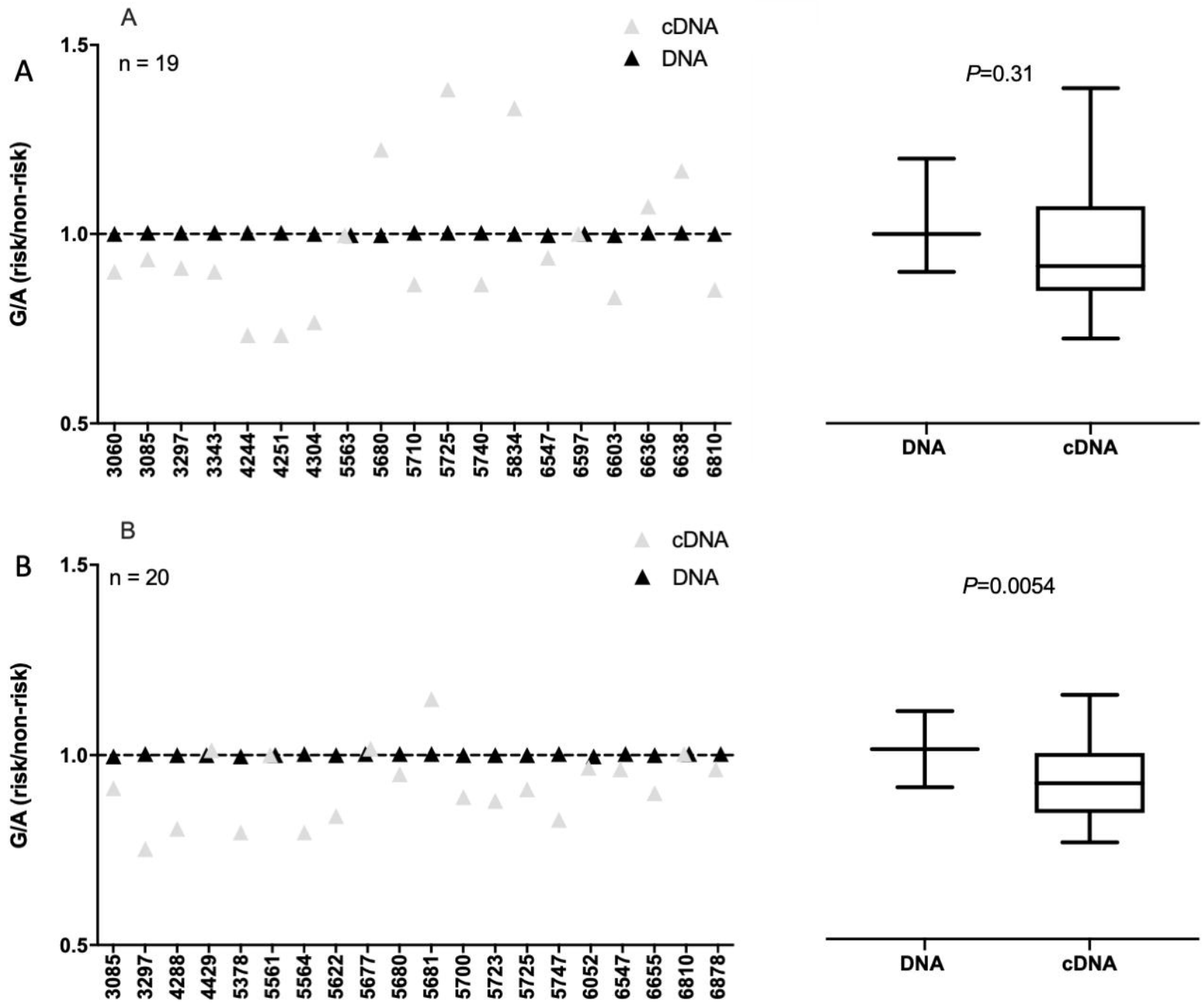
A
A
n = 19
cDNA
DNA
G/A (risk/non-risk)
1.5
1.0
0.5
3060
3085
3297
3343
4244
4251
4304
5563
5680
5710
5725
5740
5834
6547
6597
6603
6636
6638
6810
P=0.31
DNA
cDNA
B
B
n = 20
cDNA
DNA
G/A (risk/non-risk)
1.5
1.0
0.5
3085
3297
4288
4429
5378
5561
5564
5622
5677
5680
5681
5700
5723
5725
5747
6052
6547
6655
6810
6878
P=0.0054
DNA
cDNA

Figure 5

A

26bp deletion

5′ CTCCAGCAGGGAGATGAGGTTGTGGCCATCGCGGAG 3′ Control
5′ CTCCA CGGAG 3′ Deletion

B

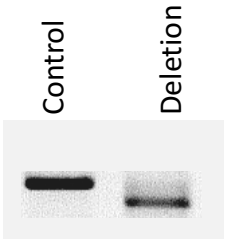

DNA

C

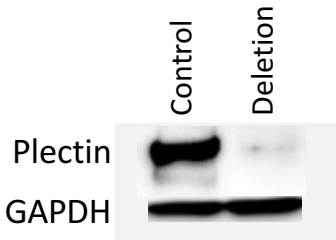

Protein

D

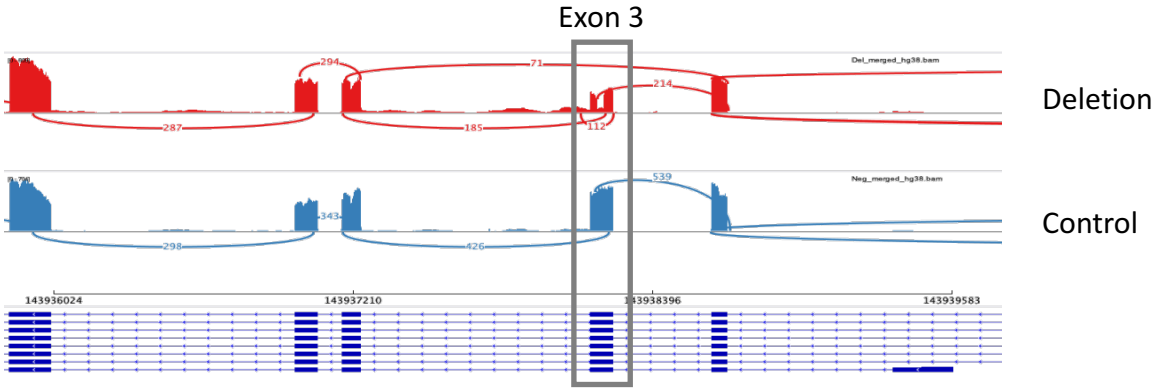

PLEC

Figure 6

A

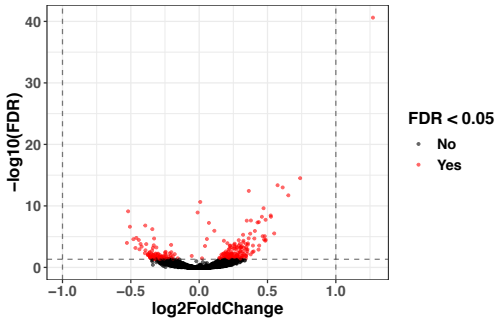

B

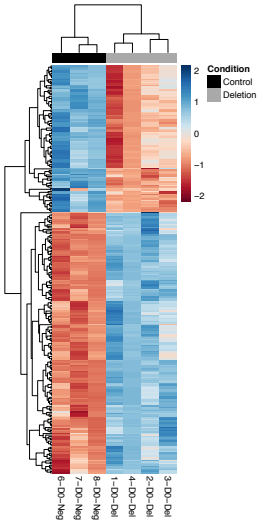

C

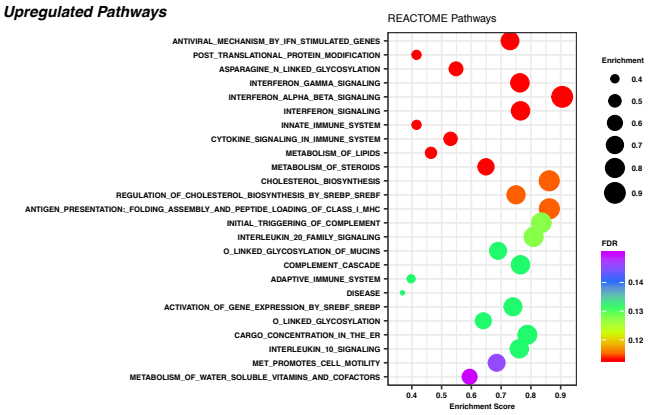
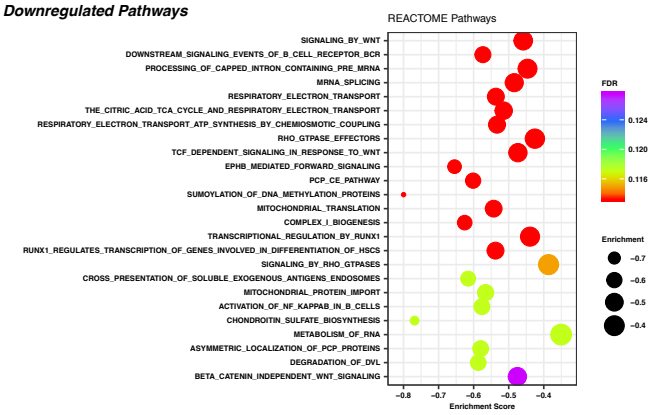
D